Fully Automatic Lung Segmentation in Thoracic CT Images using K-means Thresholding

Muhammad Basit Khan[1], Furqan Shaukat[1], Muhammad Abdullah[1]*, Junaid Mir and Gulistan Raja[1]

[1]Department of Electronic Engineering, University of Engineering & Technology, Taxila, 47080, Pakistan
abdullah6030@yahoo.com

Abstract. Lung segmentation can be considered as one of the most important steps in the Computer-Aided Diagnosis (CAD) system for lung cancer at its early stage. Accurate lung segmentation can significantly enhance the efficiency of the CAD system by removing unnecessary parts from the input image. It also helps to reduce challenges in detecting juxta-pleural nodules that show higher malignancy than the other nodule types. This paper uses advanced image processing techniques to present a fully automatic algorithm for lung segmentation of thoracic CT images. The proposed method uses K-means thresholding and various morphological operations to handle juxta-pleural nodules. Closing operation was used for hole filling which preserves objects' shape, size, and connectivity. Opening operation is applied to smooth object boundaries. The proposed method is tested on forty-two subjects with juxta-pleural nodules (approximately 7,672 CT images) taken from the publicly available dataset LIDC-IDRI. The proposed method demonstrates exceptional performance with a pixel accuracy of 97.28% and a segmentation accuracy of 97.64% based on Jaccard's index.

Keywords: Lung Segmentation, Computer-Aided Detection, K-means Thresholding, CT Image.

1 Introduction

Lung cancer is one of the most common cancers in the world, with 2.2 million new cases recorded in 2020 [1]. Approximately 225,000 people are diagnosed with lung cancer every year in the United States alone, costing $12 billion in healthcare [2][3]. Lung cancer mortality in Asia rose to an alarming figure of 926,436 out of the 1,033,881 diagnosed cases in 2012, with a dismal survival rate of 10.4% [4]. It has been one of the major threats to human life for decades. It has the highest fatality rate after being diagnosed, this particular type of cancer is responsible for the majority of cancer-related fatalities on a global scale. Another important factor that makes lung cancer the most fatal type of cancer is its five-year survival rate (17.7%), which is the lowest compared to all other cancers with the highest mortality, such as colon (64.4%), breast (89.7%), and prostate (98.9%). Early detection of lung cancer can, therefore, play a pivotal role in reducing patient mortality. However, detecting lung cancer at an early stage is challenging due to a lack of symptoms in most patients until cancer has advanced to an incurable stage. Accurately detecting and segmenting organs, such as the lung, is an essential process, particularly in the field of machine learning, to eliminate extraneous factors that are unrelated to the specific organ (for example, respiratory equipment, implants, or other medical conditions).

Accurate lung segmentation is of utmost importance as it serves as a prerequisite for nodule detection. Any inaccuracies in lung volume segmentation can significantly impact the overall

© The Author(s) 2024
I. U. Ahad (ed.), *Proceedings of the 4th International Conference on Key Enabling Technologies (KEYTECH 2024)*, Atlantis Highlights in Engineering 35,
https://doi.org/10.2991/978-94-6463-602-4_9

system's accuracy. Lung segmentation presents several challenges, primarily arising from the presence of inhomogeneities within the lung region and similar density patterns exhibited by other pulmonary structures such as veins, arteries, bronchi, and bronchioles. However, the detection of nodules attached to the pleural surface (known as juxta-pleural nodules) poses the most significant challenge for researchers. If the lung segmentation process fails to accurately define the boundaries of the lungs, there is a risk of missing these juxta-pleural nodules [5]. Hence, there is a requirement for an efficient lung segmentation technique to improve the effectiveness of computeraided detection (CAD) systems, specifically capable of accurately identifying genuine lung nodules.

In this paper, we present a fully automated method for segmenting lung volumes from CT scan images. This study introduces a new approach that uses k-means thresholding to achieve lung segmentation, accurately outlining the lung boundaries and extracting the region of interest (ROI) area. Additionally, various morphological operations are applied to correct any broken borders, ensuring the inclusion of juxta-pleural nodules while minimizing the risk of over-segmentation as in [6]. Main novelty of the work is that closing operation is used instead of dilation for hole filling and handling juxta-pleural nodules. In hole filling the closing operation has two main advantages over dilation alone. Firstly, it preserves the shape and size of the lungs and secondly it ensures object connectivity, which help in false positives reduction. Similarly, additional opening operation is used for smoothing object boundaries. As compared to deep learning methods it is less computational and a small dataset can be used to test its effectiveness. The adopted method is illustrated in Figure 1, depicting the flow diagram of the process.

2 Materials and methods

The experimental database for this study utilized the publicly available Lung Imaging Database Consortium-Image Database Resource Initiative (LIDC-IDRI). The dataset consists of 1018 cases of Lung cancer. The proposed method has been applied onto a total of 42 subjects having juxta-pleural nodules (approximately 7,672 CT slices) taken from this dataset.

2.1 Pre-processing

The purpose of pre-processing is to standardize the CT images before further analysis or lung segmentation and also to enhance accuracy. The following steps are carried out in pre-processing:

1. Normalize the image $I(x, y)$ by subtracting the mean μ and dividing it by the standard deviation $\sigma 2$. Normalization helps to bring the intensity values of the image to a similar scale, making it easier to work with and reducing the impact of variations in intensity across different images.
2. Extract the middle region of interest from the normalized image.
3. Set the pixels in the image with values equal to the maximum and minimum to the calculated mean value.
4. Apply the median filter to the image to reduce salt and pepper noise. In median filtering, a kernel of size $n \times n$ is moved over the image such that the pixel in center replaces the median of pixels in the neighborhood.

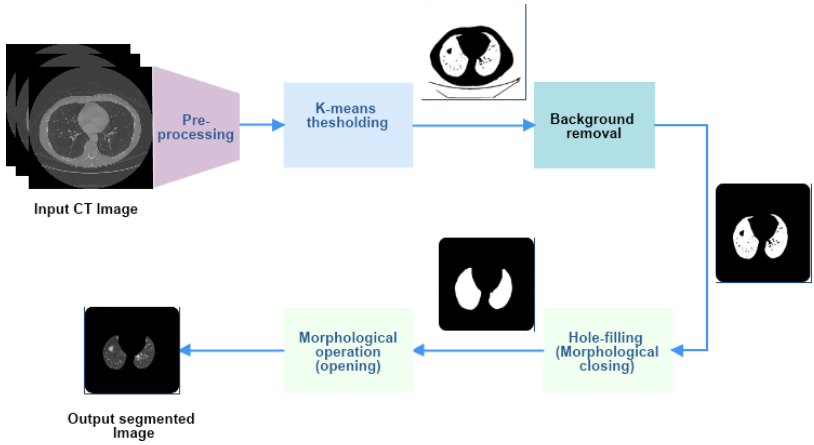

Fig.1: Flow diagram of the Proposed Method

2.2 K-Means Thresholding

K-Means thresholding, also known as K-Means-based image segmentation, is a method used to automatically determine a threshold value for separating different regions or objects in an image. This technique leverages the K-Means clustering algorithm, which is commonly used for data clustering tasks. The algorithm is summarized below.

Apply the K-Means clustering algorithm to the normalized region of interest. The algorithm assigns each pixel to one of the predefined clusters (in the proposed method, it is set to 2 clusters). Retrieve the cluster centers obtained from the K-Means clustering. These represent representative intensity values of the clusters in the region of interest. Calculate the threshold value for segmentation. The threshold value is calculated as the mean of the cluster centers.

Generate a binary mask by applying the calculated threshold to the entire image. Pixels with intensity values below the threshold are assigned one value (e.g., 1.0) to represent the foreground or object of interest, while pixels above the threshold are assigned another value (e.g., 0.0) to represent the background or other objects.

2.3 Background Removal and Hole Filling

After generating the binary mask by applying the calculated threshold to the entire image, the next step is background removal. This process combines labeling, region analysis, and the creation of a binary mask to achieve background removal or separation of foreground objects from the background in an image. Once the background is removed, a series of morphological operations are performed on the resulting image to refine the lung volume.

Erosion. Erosion erodes the boundary of the foreground objects and reduces their size. It is used to remove small protrusions or noise from the foreground.

Dilation. Dilation expands the boundaries of the foreground objects, making them more visible and connected. It can help in filling in gaps and smoothing the edges of the objects.

Closing. Closing is dilation followed by erosion. it is used for filling in small holes and gaps in the foreground regions. It is used to smooth and complete the shape of the foreground objects. It is also used for handling Juxta-Pleural Nodules. A mask containing ones of size 25×25 has been used for closing operation.

Opening: Opening is erosion followed by dilation. It is used for smoothing object boundaries and separating connected objects. A mask containing ones of size 9×9 has been

used for opening operation. Finally, the segmented lung regions are obtained by multiplying the resulting lung mask by the normalized image.

3 Results and discussion

The performance of the proposed method was evaluated on a dataset comprising 42 CT subjects, including 18 subjects with juxta-pleural nodules. This dataset consisted of approximately 7,672 CT slices obtained from the LISC-IDRI dataset. Figure 2 illustrates the sample results obtained through the proposed method's flow process. The results demonstrate that the proposed method achieved a pixel accuracy of 97.278% and a Jaccard's Index accuracy of 0.9764, which is the best among the state-of-the-art methods indicating a reduction in False positives and False negatives. Moreover, when applied to patients having juxta-pleural nodules, the proposed method effectively captured all the nodules within the Regions of Interest (ROIs). The literature provides several methods and approaches for lung segmentation, as outlined by researchers. However, only a few of these methods effectively address the challenge of juxta-pleural nodules. In Table 1, we compare the performance of the proposed method with other segmentation methods described in research articles. It should be noted that a fair comparison of methods requires the use of the same datasets and adherence to standardized image criteria. Nevertheless, our automated method consistently achieves good results and demonstrates higher segmentation accuracy when compared to other methods in general.

(a) (b) (c) (d) (e)

Fig.2. The samples of the lung segmentation of the proposed methods are as follows: (a) Original lung CT images. (b) The images after k-mean thresholding. (c) The images after the background removed (d) The images after the morphological closing operation (e) The final segmented images obtained after morphological opening.

3.1 False positives and negatives

Total average of False positives and False negatives is around 7136 pixels, while True positives and True negatives range upto 255008 pixels, which is a sign of good performance as indicated by pixel accuracy and Jaccard’s index.

Table 1. Comparison of proposed method with State-Of-The-Art methods

Author	Year	Method	PA average (%)	Jaccard's Index
Ours work	2024	**Proposed Method** k-means clustering for segmentation. Closing operation is used for hole filling and handling Juxtapleural nodules. Opening operation is used for smoothing object boundaries	97.27	0.9764
Sahu et al. [6]	2021	k-means clustering for segmentation and hole filling is done by dilation combined with intersection and complementation. Closing is used for handling Juxtapleural nodules.	97.52	0.9685
Liao et al. [7]	2016	Segmentation based on super-pixels and a self-generating neural forest	92.22	0.9207
Liu X et al. [8]	2020	KISEG (Key and Intermediate frame of Segmentation)	94.90	0.7889
Kumar et al. [9]	2021	UNet Segmentation based on super-pixels and a self-generating neural forest	98.71	0.7539
Liu X et al. [8]	2020	KISEG (Key and Intermediate frame of Segmentation)	94.90	0.7889

4 Conclusion

Lung segmentation is the crucial step in CT images to detect pulmonary diseases. The proposed method is applied to a total of 42 subjects taken from the public dataset LIDCIDRI, and among these, 18 subjects had juxta-pleural nodules. The experimental results demonstrate that our approach can effectively include all juxta-pleural nodules within the lungs' region of interest (ROI) while minimizing both over-and under-segmentation errors. The proposed method demonstrates exceptional performance with a pixel accuracy of 97.278% and a segmentation accuracy of 0.9764 based on Jaccard's index (Intersection over Union, IoU), which ensures a reduction in false positives. Although the method has not undergone clinical validation, yet this task will be completed in near future to further reduce the shortcomings in proposed method. While the proposed method successfully addresses the challenge of accurate lung segmentation, it remains necessary to test its effectiveness in dealing with severe pathologies and other pulmonary diseases and abnormalities in future studies. In Future morphological operations can be combined with State-Of-The-Art deep learning algorithms for 3d lung segmentation. Deep learning methods can be used to predict 3d structuring elements which can be utilized in morphological operations. The method can also be extended to multimodal segmentation utilizing CXR,MRI and CT scan images.

Acknowledgments. This work is part of the NRPU project#17019 entitled "EMeRALDS: Electronic Medical Records driven Automated Lung nodule Detection and cancer risk Stratification" funded by Higher Education Commission of Pakistan.

The authors also acknowledge the financial support from Erasmus+ CBHE project BIOMED5.0, funded by the European Union (Project Number: 101129077). Views and opinions expressed are however those of the author(s) only and do not necessarily reflect those of the European Union. Neither the European Union nor the granting authority can be held responsible for them.

References

1. Sung, H., Ferlay, J., Siegel, R. L., Laversanne, M., Soerjomataram, I., Jemal, A., & Bray,
2. F. (2021). Global cancer statistics 2020: GLOBOCAN estimates of incidence and mortality worldwide for 36 cancers in 185 countries. CA: a cancer journal for clinicians, 71(3), 209249.
3. Siegel, R. L., Miller, K. D., & Jemal, A. (2019). Cancer statistics, 2019. CA: a cancer journal for clinicians, 69(1), 7-34.
4. Mariotto, A. B., Robin Yabroff, K., Shao, Y., Feuer, E. J., & Brown, M. L. (2011). Projections of the cost of cancer care in the United States: 2010–2020. Journal of the National Cancer Institute, 103(2), 117-128.
5. Moore, M. A., Attasara, P., Khuhaprema, T., Le, T. N., Nguyen, T. H., Raingsey, P. P., ... & Sobue, T. (2010). Cancer epidemiology in mainland South-East Asia-past, present and future. Asian Pac J Cancer Prev, 11(Suppl 2), 67-80.
6. Chung, H., Ko, H., Jeon, S. J., Yoon, K. H., & Lee, J. (2018). Automatic lung segmentation with juxta-pleural nodule identification using active contour model and Bayesian approach. IEEE journal of translational engineering in health and medicine, 6, 1-13.
7. Sahu, S. P., Kumar, R., Londhe, N. D., & Verma, S. (2021). Segmentation of lungs in thoracic CTs using K-means clustering and morphological operations. In Advances in Biomedical Engineering and Technology: Select Proceedings of ICBEST 2018 (pp. 331-343). Springer Singapore.
8. Liao, X., Zhao, J., Jiao, C., Lei, L., Qiang, Y., & Cui, Q. (2016). A segmentation method for lung parenchyma image sequences based on superpixels and a self-generating neural forest. PloS one, 11(8), e0160556.
9. Liu, X., Wang, K., Wang, K., Chen, T., Zhang, K., & Wang, G. (2020, September). Kiseg: a three-stage segmentation framework for multi-level acceleration of chest ct scans from covid-19 patients. In International Conference on Medical Image Computing and Computer-Assisted Intervention (pp. 25-34). Cham: Springer International Publishing.
10. Kumar, S. N., Bruntha, P. M., Daniel, S. I., Kirubakar, J. A., Kiruba, R. E., Sam, S., & Pandian, S. I. A. (2021, March). Lung nodule segmentation using unet. In 2021 7th International conference on advanced computing and communication systems (ICACCS) (Vol. 1, pp. 420-424). IEEE.

Open Access This chapter is licensed under the terms of the Creative Commons Attribution-NonCommercial 4.0 International License (http://creativecommons.org/licenses/by-nc/4.0/), which permits any noncommercial use, sharing, adaptation, distribution and reproduction in any medium or format, as long as you give appropriate credit to the original author(s) and the source, provide a link to the Creative Commons license and indicate if changes were made.

The images or other third party material in this chapter are included in the chapter's Creative Commons license, unless indicated otherwise in a credit line to the material. If material is not included in the chapter's Creative Commons license and your intended use is not permitted by statutory regulation or exceeds the permitted use, you will need to obtain permission directly from the copyright holder.